

Targeting Mutant P53 (M133I-V203a-Y220C-N239Y-N268D) in Cancer: Drug Repurposing via Structure-Based Virtual Screening

Ganesh Nigade¹, Santosh Tarke², Vishal More³, Santosh Belhekar⁴

¹Department of Pharmaceutical Chemistry, PDEA's Seth Govind Raghunath Sable College of Pharmacy, Saswad, Affiliated to Savitribai Phule Pune University, Pune, Maharashtra, India

²Department of Pharmacognosy and Phytochemistry, SBSPM's B. Pharmacy College, Ambajogai, Affiliated to Dr. BAMU, Ch. Sambhaji Nagar, Maharashtra, India

³Department of Pharmaceutical Chemistry, Amrutvahini Sheti and Shikshan Vikas Sanstha's Amrutvahini College of Pharmacy, Amrutnagar, PO-Sangamner (S.K.), Tal.- Sangamner, Dist.- Ahilya Nagar, Maharashtra-422608, Affiliated to Savitribai Phule Pune University, Pune, Maharashtra, India

⁴Department of Pharmacology, Gourishankar Institute of Pharmaceutical Education & Research, Limb, Satara, Affiliated to Dr. Babasaheb Ambedkar Technological University, Lonere, Raigad, Maharashtra, India

Received: 7th Jun, 2025; Revised: 23rd Jul, 2025; Accepted: 13th Aug, 2025; Available Online: 25th Sep, 2025

ABSTRACT

The tumor suppressor protein p53 has a mutant form, p53-Y220C, which is structurally destabilized and frequently is associated with enhanced cancer progression. The present study undertook the refinement of the crystal structure of the mutant (PDB ID: 2J1X) using the server PDB-REDO, so that the model would improve its quality by the R-free value from 0.2041 to 0.1791, increasing above the 89% favorite Ramachandran residues to 95%. Structural validation ProSA-Web Z-score of -6.03 indicates reliability of the model according to the analysis of up to number ERRAT Overall Quality Factor 94.72%. Virtual screening of FDA-approved drugs applied Paritaprevir (-9.6 kcal/mol), Eribulin (-9.5), and Dutasteride (-9.3 kcal/mol) as candidates stabilizing mutant cavity. VERIFY 3D analysis confirmed refined model with 93.08% residues scoring ≥ 0.1 . These output states that the optimized p53-Y220C mutant structure is applicable for in silico drug screening paving the way for more experimental validation of repurposed drug candidates.

Keywords: p53-Y220C mutant, structural refinement, virtual screening, molecular docking, drug repurposing, PDB-REDO, ProSA-Web, ERRAT, VERIFY 3D

How to cite this article: Ganesh Nigade, Santosh Tarke, Vishal More, Santosh Belhekar. Targeting Mutant P53 (M133I-V203a-Y220C-N239Y-N268D) in Cancer: Drug Repurposing via Structure-Based Virtual Screening. International Journal of Drug Delivery Technology. 2025;15(3):1228-36. doi: 10.25258/ijddt.15.3.43

Source of support: Nil.

Conflict of interest: None

INTRODUCTION

TP53 is one of the most studied of the tumor suppressor genes, and is often referred to as the world's most important guardian of the genome. This gene plays an important role in the regulation of cell cycle progression, DNA repair, apoptosis, senescence, and other functions responsible for holding the balance between genomic stability and environmental cell stress¹. The p53 is maintained at low levels under normal physiological conditions by virtue of its interaction with Murine Double Minute 2 (MDM2), an E3 ubiquitin ligase that targets p53 for proteasomal degradation².

After DNA damage or oncogenic stress, p53 stabilization and activation occurs, resulting in the transcriptional regulation of target genes involved in cell cycle arrest (e.g., p21 CIP1/WAF1)³, apoptosis (e.g., BAX, PUMA)⁴, and DNA repair (e.g., GADD45)⁵.

Mutations of the TP53 gene are present in about 50% of human cancers causing the loss of tumor suppressor function. These mutations are categorized into three classes, which are loss-of-function (LOF), dominant-negative (DN), and gain-of-function (GOF). LOF mutations abolish the

functional capacity of p53 to regulate expression of its targeted genes, whilst DN mutations interfere with the function of the wild-type (WT) allele⁶. GOF mutations acquire an oncogenic capability in p53 that cause excessive growth, resistance to apoptosis, and genotoxic instability. The important effect of mutated p53 on tumor progression highlights the need for new therapeutic strategies to restore mutant allele expression or remove cancers expressing mutant p53.

The mutations in TP53 found in the human cancers led us to the Y220C mutation as the one possessing striking structural consequences and therapeutic potential. Substitution of cysteine (C) for tyrosine (Y) at position 220 triggers loss of structural integrity of the DNA-binding domain and the creation of a surface-exposed cavity in the protein. This destabilizes the mutant protein, allowing partial unfolding at physiological temperatures and subsequent loss of DNA binding and additional transcriptional regulatory functions by way of the latter mutation⁷.

This mutation affects the stability of the protein, which has affected the conformation of p53 rather than impinging

Table 1: Receptor-based Screen Summary

Name	Score	MW	HBD	HBA	RB	NOA	Rings	LogP
Paritaprevir	-9.6	765.89	3	9	9	14	8	4.6
Eribulin	-9.5	729.908	2	2	5	12	9	1.1
Dutasteride	-9.3	528.5297	2	2	3	4	5	6.5
Fluspirilene	-9.2	475.5727	1	1	7	4	5	5.9
Ubrogepant	-9.2	549.554	2	5	5	8	6	3.1
Entrectinib	-9.2	560.65	2	2	8	8	6	5.7
Fluorescein	-9.1	332.3063	2	3	2	5	5	3.4
Elexacaftor	-9.1	597.66	1	6	9	11	4	4.8
Digitoxin	-9.0	764.9391	5	6	12	13	8	2.8
Aprepitant	-9.0	534.4267	0	2	6	7	4	6.0
Abemaciclib	-9.0	506.606	1	4	7	8	5	3.8
Dexamethasone	-8.9	576.63	3	8	9	9	5	2.4
Tucatinib	-8.9	480.532	2	4	6	10	6	3.9
Dihydroergotamine	-8.9	583.6774	2	4	6	10	8	2.3
Leucovorin	-8.8	473.446	6	8	13	14	3	0.5
Pimozide	-8.8	461.5462	0	1	7	4	5	6.9
Digoxin	-8.8	780.9385	6	7	13	14	8	1.6
Regorafenib	-8.8	482.815	3	3	8	7	3	4.1
Eltrombopag	-8.8	442.4666	3	4	7	8	4	4.7
Dihydroergocristine	-8.8	611.743	2	4	7	10	8	3.3
Lumacaftor	-8.7	452.414	2	4	7	7	5	4.4
Levoleucovorin	-8.7	473.4393	6	8	13	14	3	0.5
Linagliptin	-8.7	472.5422	1	5	5	10	5	3.8
Sorafenib	-8.7	464.825	3	3	8	7	3	4.0
Pazopanib	-8.7	437.518	2	5	5	9	4	3.0
Meprednisone	-8.7	372.461	2	5	4	5	4	1.9
Prednisone	-8.6	358.4281	2	5	4	5	4	1.5
Ergotamine	-8.6	581.6615	2	4	6	10	8	2.0
Betamethasone	-8.6	472.446	4	7	8	8	4	0.3
Telmisartan	-8.6	514.6169	1	4	8	6	6	6.9
Steviolbioside	-8.6	642.739	8	9	15	13	6	0.6
Avapritinib	-8.6	498.57	1	5	5	10	6	1.8
Ponatinib	-8.6	532.5595	1	3	6	7	5	4.1
Phenolphthalein	-8.6	318.3228	2	3	4	4	4	3.8
Drospirenone	-8.6	366.4932	0	2	0	3	7	3.5
Glimepiride	-8.5	490.62	3	5	11	9	3	3.8
Paliperidone	-8.5	426.4839	1	4	5	7	5	3.3
Tezacaftor	-8.5	520.505	4	4	12	8	5	2.9
Bictegravir	-8.5	449.386	2	4	5	8	5	3.5
Lurasidone	-8.5	492.676	0	3	5	6	7	5.3
Ibrutinib	-8.5	440.507	1	4	6	8	5	3.5
Alloin	-8.4	418.398	7	8	10	9	4	-0.1
Dolutegravir	-8.4	419.3788	2	4	5	8	4	3.2
Mizolastine	-8.4	432.503	0	3	5	7	5	5.2
Clozapine	-8.3	326.823	1	0	1	4	4	3.0
Alpelisib	-8.3	441.47	2	4	6	7	3	3.2
Risperidone	-8.3	410.4845	0	3	4	6	5	4.4
Piritramide	-8.3	430.5851	1	2	7	5	4	3.6
Ceftobiprole	-8.3	534.57	5	8	9	14	5	-2.4
Ceritinib	-8.3	558.135	3	4	9	8	4	6.4
Plerixafor	-8.3	502.782	6	0	4	8	3	-0.0
Levocabastine	-8.3	420.528	1	3	5	4	4	2.5
Reserpine	-8.2	608.6787	0	2	10	11	6	4.0
Adapalene	-8.2	412.5201	1	2	5	3	6	7.7
Fluoxymesterone	-8.2	336.4409	2	3	2	3	4	2.1
Tolvaptan	-8.2	448.941	2	3	6	5	4	4.7
Imatinib	-8.2	493.6027	2	4	8	8	5	3.5
Loripirazole	-8.2	405.469	0	2	4	5	5	3.3

Table 1: Receptor-based Screen Summary

Name	Score	MW	HBD	HBA	RB	NOA	Rings	LogP
Difenoxin	-8.2	424.5341	1	3	8	4	4	2.7
Olaparib	-8.2	434.4628	0	4	6	7	5	3.5
Ulobetasol	-8.2	428.9	2	4	4	4	4	2.6
Methyltestosterone	-8.2	302.451	1	2	1	2	4	3.5
Maraviroc	-8.2	513.6655	1	3	9	6	5	5.1
Clofazimine	-8.2	473.396	1	1	4	4	5	8.6
Atovaquone	-8.2	366.837	1	3	3	3	4	5.6
Nilotinib	-8.2	529.5158	2	5	7	8	5	4.9
Cloxacillin	-8.2	435.881	2	5	6	8	4	2.5
Clobetasol	-8.1	410.907	2	4	4	4	4	2.7
Clobetasone	-8.1	408.89	1	4	3	4	4	2.7
Grazoprevir	-8.1	766.903	3	8	10	15	7	4.7
Domperidone	-8.1	425.911	0	2	5	7	5	5.4
Indigotindisulfonic acid	-8.1	422.389	4	8	4	10	4	0.5
Rucaparib	-8.1	323.371	2	1	3	4	4	2.4
Palonosetron	-8.1	296.414	0	1	1	3	5	2.7
Ziprasidone	-8.1	412.936	1	2	4	5	5	4.0
Halcinonide	-8.1	454.96	1	3	3	5	5	2.7
Hydrocortisone	-8.1	362.4599	3	5	5	5	4	1.6
Mefloquine	-8.1	378.3122	2	2	3	3	3	3.6
Dihydroergocornine	-8.1	563.699	2	4	6	10	7	2.7
Riociguat	-8.1	422.4157	2	5	6	10	4	1.5
Duvelisib	-8.1	416.87	1	4	4	7	5	5.4
Dabrafenib	-8.0	519.562	2	5	6	7	4	4.7
Perampanel	-8.0	349.393	0	3	3	4	4	5.1
Cefpirome	-8.0	514.577	2	5	7	11	5	2.3
Dicoumarol	-8.0	336.295	2	4	4	6	4	1.6
Indoramin	-8.0	347.4534	1	1	6	4	4	3.8
Bromocriptine	-8.0	654.595	2	4	7	10	7	3.7
Oxatomide	-8.0	426.564	0	1	7	5	5	5.4
Talazoparib	-8.0	380.359	1	4	2	7	5	3.6
Fluocinonide	-8.0	494.5249	1	4	5	7	5	2.1
Bisoxatin	-7.9	333.343	3	3	4	5	4	3.3
Etoposide	-7.9	588.5566	3	4	8	13	7	1.0
Betamethasone	-7.9	392.4611	3	5	5	5	4	2.0
Terfenadine	-7.8	471.6734	2	2	11	3	4	6.5
Vemurafenib	-7.7	489.922	1	4	7	6	4	4.9
Flunarizine	-7.7	404.4948	0	0	6	2	4	5.6
Fosaprepitant	-7.7	614.4066	2	5	9	10	4	2.7
Macimorelin	-7.6	474.565	4	3	12	9	4	2.2
Hydrocortisone cypionate	-7.4	486.649	2	5	9	6	5	4.1
Metergoline	-7.3	403.526	1	1	6	5	5	3.7

directly upon its DNA interaction. Therefore, owing to the destabilization, the mutant p53 will tend to aggregate and will subsequently undergo degradation that would further incapacitate its tumor-suppressive functions. Due to this uniqueness associated with the stabilizing conformation, p53-Y220C serves as an ideal target for small-molecule stabilizers that could restore its functional conformation to regain its normal function of regulating target genes⁸.

It has been shown that many pharmacological chaperones or small molecules bind selectively to the newly exposed hydrophobic cavity resulting from the Y220C mutation, stabilizing the mutant protein and rescuing its tumor-suppressive activity. This is an interesting opportunity for

drug discovery, particularly in drug repurposing by screening for new applications for existing FDA-approved drugs⁹.

Drug repurposing or repositioning stands as a time- and cost-saving shortcut for the identification of new therapeutic uses for drugs that have already been approved. Compared to de novo drug discovery, which takes a long time and lots of money, drug repurposing has its own benefits. Medicines under repurposing have already undergone a wide range of assessments on safety and pharmacokinetics; hence, they can go beyond early preclinical trials and enter clinical trial phases for new indications, leading to shortened development time.

Furthermore, drug repurposing helps to mitigate R&D costs, as these drugs already have well-characterized pharmacodynamic and toxicological profiles. Lastly, repurposed drugs have been shown to be safe for humans, giving a higher chance of getting approved by regulatory authorities regarding new indications¹⁰.

Structure-Based Virtual Screening (SBVS) is one of the most exciting methodologies for drug repurposing in oncology. In this context, it refers to in silico screening of large libraries of FDA-approved drugs for a given target protein structure in order to find possible binders. On the positive side, SBVS allows high precision targeting using high-resolution crystallographic structures to identify small molecules fitting the exposed cavity of the mutant protein, thus stabilizing and restoring its function. Second, SBVS allows the rapid screening of thousands of compounds, thereby accelerating the process of promising drug candidate identification. Third, SBVS is also cheaper than classical HTS: since it uses computational predictions to direct most resources to the high-affinity binders, it diminishes resource usage by all hits that do not fit this description¹¹.

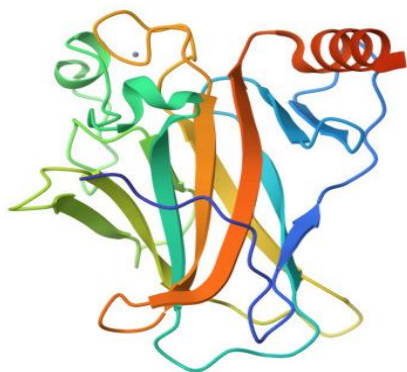


Figure 1: Protein structure of p53-Y220C mutant (PDB ID: 2J1X)

Researchers could integrate drug repurposing with SBVS and successfully identify candidate drugs suitable for stabilizing mutant p53-Y220C, as it is an important target in p53-mutant cancers. Such paradigms shift in cancer therapeutics, now leading personalized and precision medicine strategies for patients with malignancies driven by p53.

In this study, we harness a structure-based virtual screening approach which aims to identify FDA-approved drugs that can target the mutant p53 (M133L-V203A-Y220C-N239Y-N268D) and their therapeutic potential to be used in the context of cancer treatment. This is also relevant to the ongoing developments in the mutant p53-targeted drug discovery space with several new rationalization opportunities available for drug repurposing in oncology.

METHODS

Selection of p53-Y220C Structure for Virtual Screening

For virtual screening and molecular dynamics studies, the fully resolved crystal structure of p53-Y220C (PDB ID: 2J1X) was obtained from the Protein Data Bank. The disorder introduced by this mutation, which creates a surface cavity on p53, was analyzed via structural superimposition of wild-type and mutant forms to determine conformational changes¹².

Improvement of Quality with PDBredo Server

Then structural refinement was done using the PDBredo server to increase structural accuracy of the retrieved p53-Y220C model. This tool optimizes the crystallographic structure by improving the position of atoms, correcting errors, and refining bond geometries¹³. The refined structure ensures that docking studies are carried out with a high-quality protein model, rendering more reliable predictions of drug interactions¹⁴.

Quality Check by SAVES and ProSA Server

After refinement, the p53-Y220C structure was subjected to validation from computational quality assessment methods

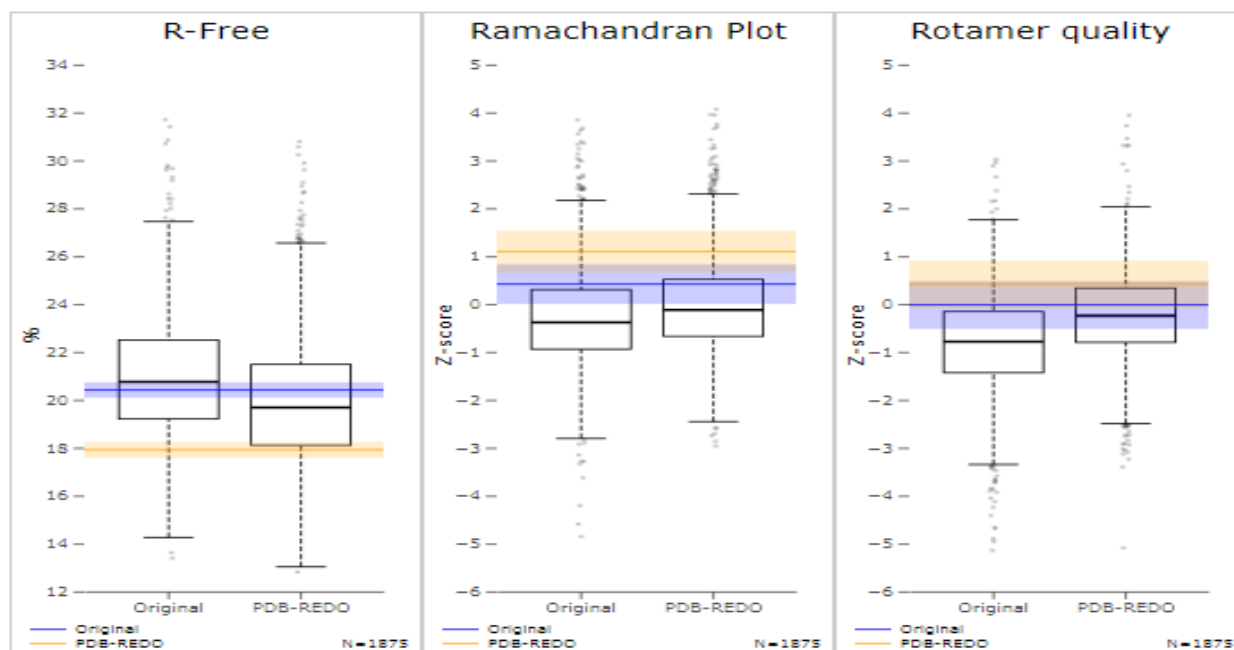


Figure 2: Model quality compared to resolution neighbours

such as SAVES and ProSA servers. The SAVES (Structure Analysis and Verification Server) checked the model for structural errors and verified its stereochemical quality, thus ensuring it achieved structural integrity criteria¹⁵. The ProSA (Protein Structure Analysis) server analyzed the energy profile of the structure and overall quality, thereby corroborating its suitability for virtual screening¹⁶.

Receptor-Based Virtual Screening of FDA Approved Drugs by DrugRep

FDA-approved drugs that can bind to and help stabilize p53-Y220C were identified by an in silico screening strategy. The DrugRep software, a specific application for drug repurposing, was used to dock with its library FDA approved drugs onto the mutant version of the p53 structure¹⁷. Each candidate was docked into the mutant p53 cavity by using molecular docking to examine binding energy and interaction strength. The high-scoring compounds indicating strong binding potential were selected for subsequent investigation¹⁸.

Cross Validation of Results of Receptor-Based Virtual Screening by Molecular Docking Studies

For confirming the output of receptor-oriented virtual screening, molecular docking studies were performed using the CB-Dock2 server. The selected ligand molecules were docked with the structure of p53-Y220C mutant (PDB ID: 2J1X) for the evaluation of their binding interactions and stability¹⁹. The docking methodology involved receptor preparation: automatic cavity detection and energy minimization; ligand preparation: optimization and conformer generation; and docking simulation using CB-Dock2 due to the specific nature of the docking. Binding affinities, hydrogen bonding, and essential molecular interactions facilitated verification of the consistency of virtual screening outcomes. This cross-validation ensured the reliability of potential lead compounds for further experimental validation²⁰.

RESULTS AND DISCUSSION

Results of Protein Data Bank (PDB) Selection and Structural Analysis of p53-Y220C Mutation

The structural analysis of p53-Y220C mutant (PDB ID: 2J1X), as can be seen in figure 1, shows that the Y220C

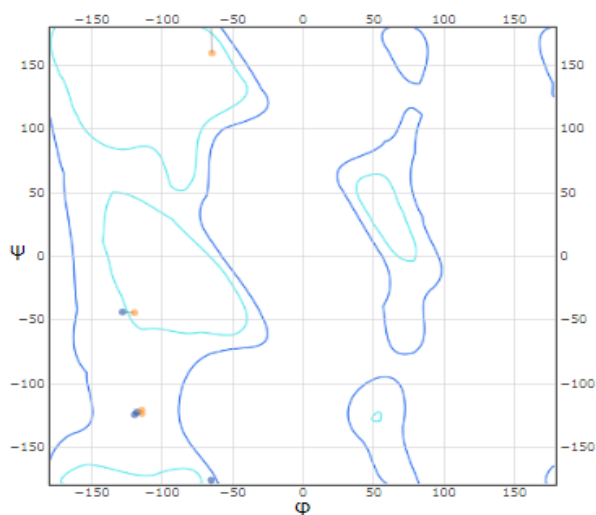


Figure 3: Kleywegt-like plot

Table 2: Results of Receptor-Based Virtual Screening by Molecular Docking Studies

Name	Score of Virtual Screening	Score of Cb-Dock-2 Docking
Paritaprevir	-9.6	-9.8
Eribulin	-9.5	-9.7
Dutasteride	-9.3	-9.4
Fluspirilene	-9.2	-9.3
Ubrogepant	-9.2	-9.3
Entrectinib	-9.2	-9.3
Fluorescein	-9.1	-9.4
Elexacaftor	-9.1	-9.2
Digitoxin	-9.0	-9.2
Aprepitant	-9.0	-9.1

mutation has been responsible for substantial conformational changes, creating a destabilizing surface cavity with the wild type p53 superimposed. The alterations in secondary and tertiary structures, in conjunction with the insensitivity of some areas, further underscore this. Computational validation confirmed the reliability of the model in drug screening. These findings augured well in selecting stabilizing drug candidates for targeting the mutation-induced cavity.

Improvements in Quality by PDBredo Server

The PDB-REDO refinement transformed the crystallographic model close to human p53 core domain mutant (PDB entry 2J1X) very significantly, with the R-free reducing from 0.2041 to 0.1791, and the bond geometry improvements as seen in figure 2 and figure 3. The refined structure showed enhanced model quality, whereby Ramachandran plot normality increased from 89 to 95, and improved rotamer normality was observed from 89 to 94. The major changes included optimization of eight rotamers, removal of 24 waters, and better fitting of residues with respect to electron density. In addition, repurposing analysis using CB-Dock found out five possible binding pockets for the drugs discovered- most of which pocket 1 is highlighted, owing to its interaction with the residues like LEU264, LYS101, and ARG267. Well optimization has therefore been achieved for future drug screening and analysis of structures that show much more superior quality and reliability for computational and experimental studies.

Quality Check by SAVES and ProSA Server

ProSA-Web Analysis of p53-Y220C Mutant (PDB ID: 2J1X)

The Z-score of -6.03 therefore has confirmed the p53-Y220C mutant structure among experimentally determined protein structures in the Protein Data Bank (PDB). The Z-score plot places the model in the expected distribution of native proteins of similar size, confirming it as reliable for further computational studies (Figure 4).

The local model quality assessment (Figure 5) depicts energy levels at residue levels along the amino acid sequence. The major share of the residues were found to have a negative energy value, which indicated good structural stability. Contrasting the data by smoothing it over 40 residue windows showed that there was only very little fluctuations, suggesting that the model is free of major structural irregularities. The smaller window of 10 residues

(background line) corroborated that observation by providing finer resolution of local quality, asserting that no truly problematic areas exist within structure.

Jmol viewer. Interactive 3D rendering of the protein structure color-coded by residue energy (figure 6). The blue-to-red gradient represents stable to less stable regions, while the majority of residues fall into the stable (blue) to moderate stable (green/yellow) range. Thus, the structural integrity of the model is retained; this lends credibility to its use for molecular docking and dynamics simulations.

Hence, the ProSA-Web analysis confirms that the p53-Y220C mutant structure (PDB ID: 2J1X) is overall very well characterized with respect to its quality: Z-score is in the acceptable range, the residue energy distribution is stable, and deviations in the protein structures are minimal. Thus, all these encouraging results may indicate that the model can successfully be used for further computations,

such as ligand binding and stability checks in drug discovery research.

The Ramachandran plot analysis of the p53-Y220C mutant (PDB ID: 2J1X) proved that the structural quality is very high, with 90.4% of residues lying in the most favored regions and 9.6% in additionally allowed regions, while no residues were found in generously allowed or disallowed regions. Of the 390 total residues, 332 were non-glycine and non-proline residues, with 26 of these being glycine and 28 proline residues. Those results were consistent with expectations for high-resolution protein structures and confirm that the model shows the stereochemical quality and applicability for future computational studies. Figure 7 gives a picture of the Ramachandran plot.

Error analysis showed an overall quality factor of 94.72, indicating that it is a highly reliable protein structure with the least errors regarding non-bonded atomic interactions.

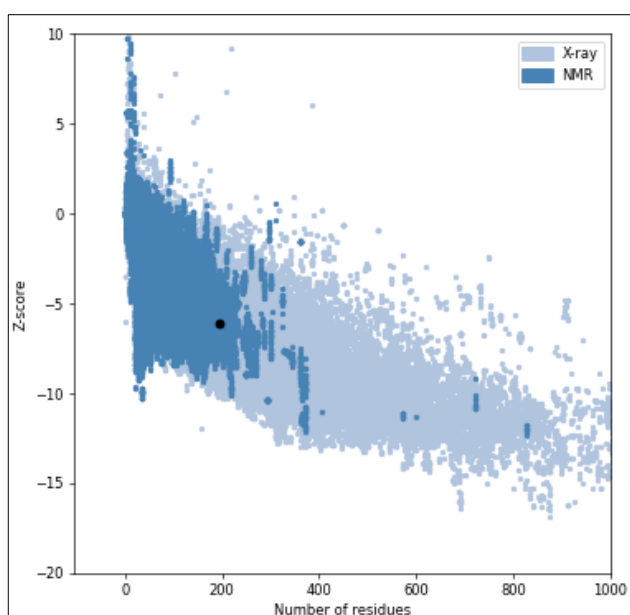


Figure 4: Overall Model Quality (Z-Score)

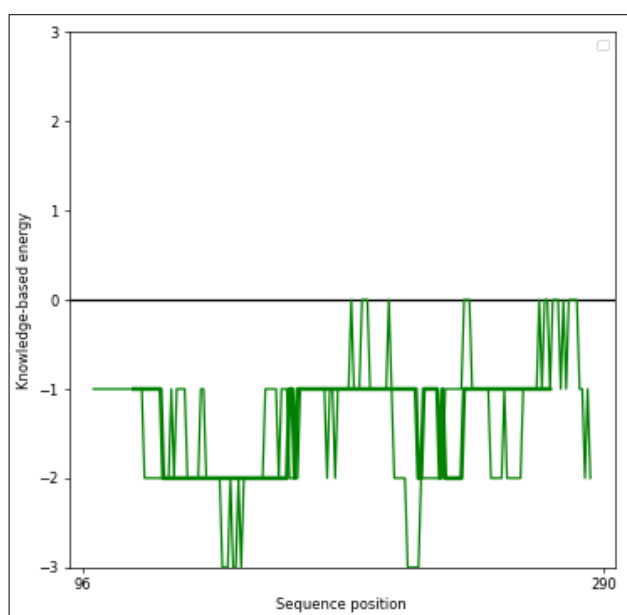


Figure 5: Local Model Quality (Residue Score Plot)

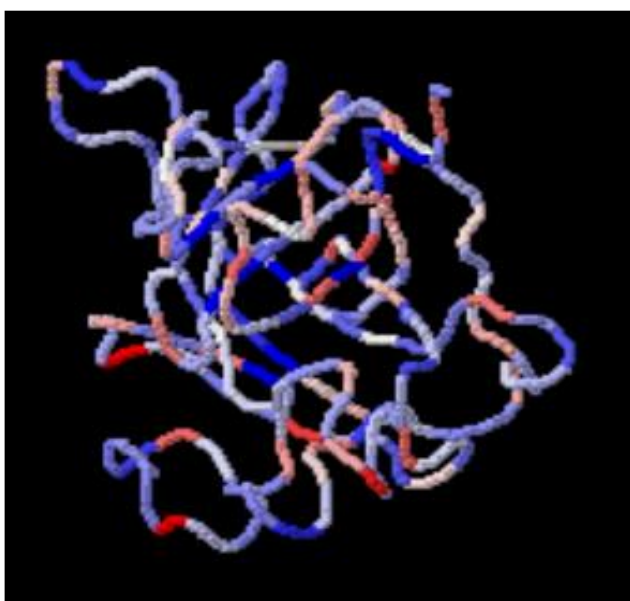


Figure 6: 3D Structure Visualization (Jmol)

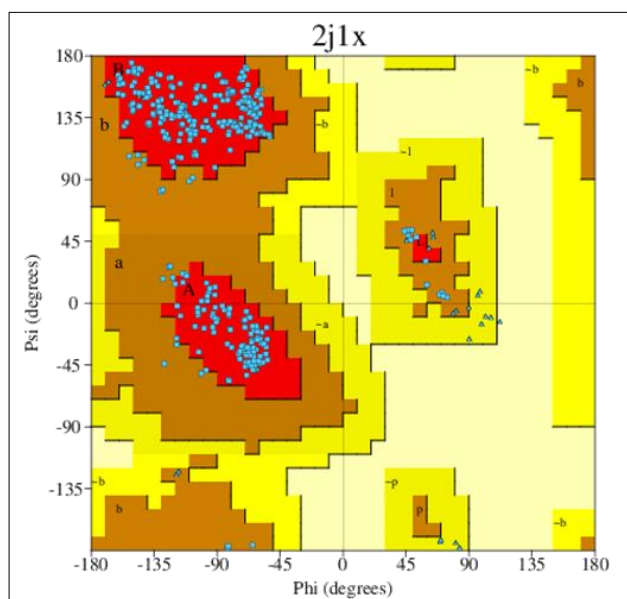


Figure 7: The Ramachandran plot

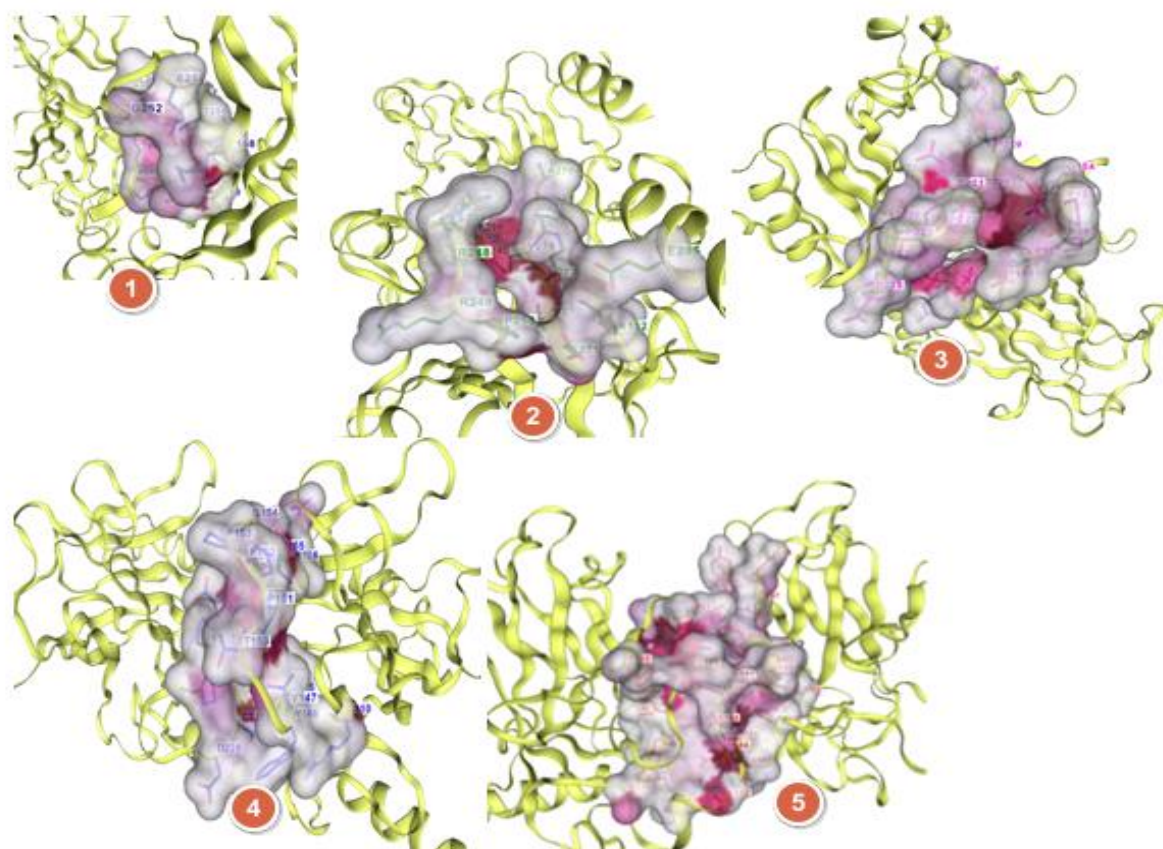


Figure 8: Cavities found in p53-Y220C Mutant (PDB ID: 2J1X)

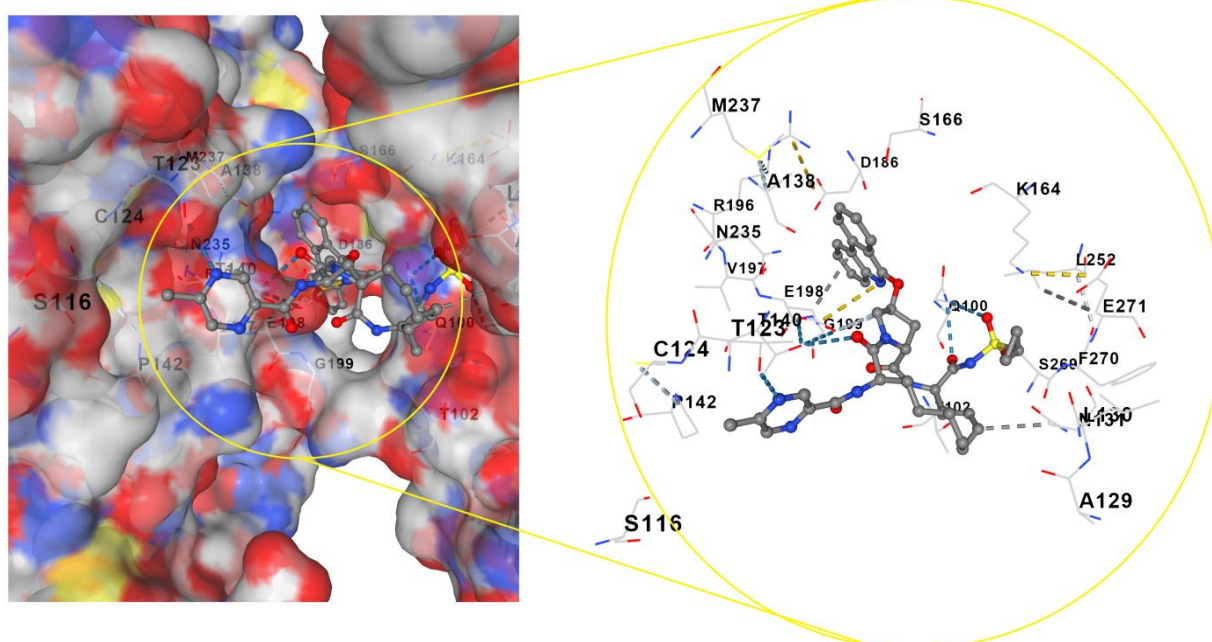


Figure 9: Interaction between Paritaprevir and p53-Y220C Mutant (PDB ID: 2J1X)

The VERIFY 3D program confirmed that 93.08% of residues scored ≥ 0.1 in the 3D/1D profile, while a minimum of 80% is required for a structurally valid model. All these results show that the p53-Y220C mutant structure has maintained good stereochemical quality and the prospect of being employed for further computational studies such as molecular docking and dynamics simulations.

Receptor-Based Virtual Screening by DrugRep

The structure-based virtual screening results presented in Table 1 provide an encouraging outlook for repurposing FDA-approved drugs for the mutant p53 (M133L-V203A-Y220C-N239Y-N268D) variant in cancer. Among the investigated compounds, paritaprevir had the best binding affinity (-9.6 kcal/mol) and appears to interact optimally

with the binding site of the mutant p53. The drug might stabilize the conformation of mutant protein due to its big size (765.89 Da) and long flexible structure with multiple (9) hydrogen bond donors and (14) hydrogen bond acceptors.

Other candidates of interest include Eribulin (-9.5 kcal/mol) and Dutasteride (-9.3 kcal/mol), which have also exhibited good binding energies suggesting their potential role in the modulation of mutant p53 function. Fluspirilene, Ubrogepant, and Entrectinib (-9.2 kcal/mol each) interacted well in molecular simulations and thus are promising candidates for repositioning. Furthermore, Fluorescein (-9.1 kcal/mol) and Elexacaftor (-9.1 kcal/mol) also scored high in docking, making them suitable candidates for experimental evaluation.

Digitoxin (-9.0 kcal/mol), a well-explored cardiac glycoside, and Aprepitant (-9.0 kcal/mol), an NK1 receptor antagonist, offer promising binding affinities for disrupting mutant p53-oncogenic pathways. These two are suggested to have exciting options for repurposing these agents with dissimilar pharmacological profiles towards restoring p53 tumor suppressor function.

Overall, the findings highlight the drug repurposing potential for identifying candidate molecules likely to be clinically relevant in targeting mutant p53 (M133L-V203A-Y220C-N239Y-N268D) in cancer. In the future, the establishment of their efficacy in restoring p53 function and inhibiting tumor growth will require molecular dynamics simulations and *in vitro* studies.

Cross Validation of Results of Receptor-Based Virtual Screening by Molecular Docking Studies

The cross-validation of receptor-based virtual screening results using CB-Dock2 molecular docking confirmed the strong binding potential of the selected repurposed drugs against the p53-Y220C mutant (PDB ID: 2J1X) cavities are provided in figure 8. The docking scores given in table 2 obtained from CB-Dock2 closely aligned with the initial virtual screening results, with Paritaprevir (-9.8 kcal/mol), Figure 9 gives Interaction between Paritaprevir and p53-Y220C Mutant (PDB ID: 2J1X) and Eribulin (-9.7 kcal/mol) showing the highest affinities, indicating strong and stable interactions. Other compounds, such as Dutasteride, Fluspirilene, and Ubrogepant, also showed comparable binding scores, reinforcing their candidacy for further studies. Such close correlation between the two methods suggests that the computational screening should be reliable and further strengthen the rationale for the experimental evaluation of such compounds in targeting mutant p53-driven cancers²¹.

CONCLUSION

The structural analysis of the mutant p53-Y220C (2J1X) depicted significant conformational changes, along with a destabilizing surface cavity that could be targeted for drug stabilization. The refinement was carried out by the PDB-REDO server which improved the quality of the model, giving an R-free value from 0.2041 to 0.1791 with a Ramachandran plot normality percentage improved from 89% to 95%. The model was confirmed as reliable by the ProSA-Web analysis, yielding a Z-score of -6.03, indicating

its consistency with the experimentally resolved protein structures. The Ramachandran plot analyzed showed validation at 90.4% for structural accuracy of residues, which did indeed fall into the favored regions.

In receptor-based virtual screening, Paritaprevir (-9.6 kcal/mol), Eribulin (-9.5 kcal/mol), and Dutasteride (-9.3 kcal/mol) were identified as the top-scoring drug candidates, indicating that these compounds are capable of strong binding to the mutation-induced cavity. Furthermore, the model was confirmed as highly reliable by ERRAT analysis, obtaining an Overall Quality Factor of 94.72, while a VERIFY 3D analysis of the model indicated that 93.08% of residues scored ≥ 0.1 , which is above the accepted standard of 80%.

All findings taken into account suggest that this refined p53-Y220C mutant model has been properly optimized for drug screening, yielding exciting candidates for drug repurposing to be validated by molecular dynamics simulations and experimental work.

REFERENCES

- Patil MR, Bihari A. A comprehensive study of p53 protein. *Journal of Cellular Biochemistry*. 2022 Dec;123(12):1891-937. <https://doi.org/10.1002/jcb.30331>
- Chinnam M, Xu C, Lama R, Zhang X, Cedeno CD, Wang Y, Stablewski AB, Goodrich DW, Wang X. MDM2 E3 ligase activity is essential for p53 regulation and cell cycle integrity. *PLOS Genetics*. 2022 May 19;18(5):e1010171. <https://doi.org/10.1371/journal.pgen.1010171>
- Cutty SJ, Hughes FA, Ortega-Prieto P, Desai S, Thomas P, Fets LV, Secrier M, Barr AR. Pro-survival roles for p21 (Cip1/Waf1) in non-small cell lung cancer. *British Journal of Cancer*. 2024 Dec 20;1-7. <https://doi.org/10.1038/s41416-024-02928-9>
- Wang J, Thomas HR, Li Z, Yeo NC, Scott HE, Dang N, Hossain MI, Andrabi SA, Parant JM. Puma, noxa, p53, and p63 differentially mediate stress pathway induced apoptosis. *Cell Death & Disease*. 2021 Jun 30;12(7):659. <https://doi.org/10.1038/s41419-021-03902-6>
- Palomer X, Salvador JM, Griñán-Ferré C, Barroso E, Pallàs M, Vázquez-Carrera M. GADD45A: With or without you. *Medicinal Research Reviews*. 2024 Jul;44(4):1375-403. <https://doi.org/10.1002/med.22015>
- Chen X, Zhang T, Su W, Dou Z, Zhao D, Jin X, Lei H, Wang J, Xie X, Cheng B, Li Q, Zhang H, Di C. Mutant p53 in cancer: From molecular mechanism to therapeutic modulation. *Cell Death & Disease*. 2022 Nov 18;13(11):974. <https://doi.org/10.1038/s41419-022-05408-1>
- Gener-Ricos G, Bewersdorf JP, Loghavi S, Bataller A, Goldberg AD, Sasaki K, Famulare C, Takahashi K, Issa GC, Borthakur G, Kadia TM, Short NJ, Senapati J, Carter BZ, Patel KP, Kantarjian H, Andreeff M, Stein EM, DiNardo CD. TP53 Y220C mutations in patients with myeloid malignancies. *Leukemia & Lymphoma*. 2024 Aug 23;65(10):1511-5. <https://doi.org/10.1080/10428194.2024.2363440>

8. Chasov V, Davletshin D, Gilyazova E, Mirgayazova R, Kudriaeva A, Khadiullina R, Yuan Y, Bulatov E. Anticancer therapeutic strategies for targeting mutant p53-Y220C. *Journal of Biomedical Research*. 2024 May;38(3):222-32. <https://doi.org/10.7555/JBR.37.20230093>
9. Stephenson Clarke JR, Douglas LR, Duriez PJ, Balourdas DI, Joerger AC, Khadiullina R, Bulatov E, Baud MG. Discovery of nanomolar-affinity pharmacological chaperones stabilizing the oncogenic p53 mutant Y220C. *ACS Pharmacology & Translational Science*. 2022 Oct 11;5(11):1169-80. <https://doi.org/10.1021/acspsci.2c00164>
10. Hua Y, Dai X, Xu Y, Xing G, Liu H, Lu T, Chen Y, Zhang Y. Drug repositioning: Progress and challenges in drug discovery for various diseases. *European Journal of Medicinal Chemistry*. 2022 Apr 15;234:114239. <https://doi.org/10.1016/j.ejmech.2022.114239>
11. Sohraby F, Aryapour H. Rational drug repurposing for cancer by inclusion of the unbiased molecular dynamics simulation in the structure-based virtual screening approach: Challenges and breakthroughs. *Seminars in Cancer Biology*. Academic Press. 2021 Jan 1;68:249-57. <https://doi.org/10.1016/j.semcancer.2020.04.007>
12. Han IS, Thayer KM. Reconnaissance of allostery via the restoration of native p53 DNA-binding domain dynamics in Y220C mutant p53 tumor suppressor protein. *ACS Omega*. 2024 Apr 22;9(18):19837-47. <https://doi.org/10.1021/acsomega.3c08509>
13. Bethi S, Shirole R, More V, Thorat M, Mohapatra S, Tare H. Uncovering the anticonvulsant mechanisms of Saussurea Lappa: A network pharmacology and molecular docking approach. *Palestinian medical and pharmaceutical journal*. 2025 Jan 1;9999(9999):None-(Pal. Med. Pharmaceutical Journal)
14. de Vries I, Perrakis A, Joosten RP. PDB-REDO in computational-aided drug design (CADD), Open Access Databases and Datasets for Drug Discovery. (edited by: A Daina, M Przewosny & V Zoete). John Wiley & Sons: Chichester. 2024 Feb 5:201-29. <https://doi.org/10.1002/9783527830497.ch7>
15. Gholipour Z, Fooladi AA, Parivar K. Targeted therapy with a novel superantigen-based fusion protein against interleukin-13 receptor $\alpha 2$ -overexpressing tumor cells: An in-silico study. *Iranian Journal of Pathology*. 2024 Feb 15;19(2):193-204. <https://doi.org/10.56042/ijnpr.v15i4.9059>
16. Bethi S, Shirole R, Ghangale G. Computational exploration of multitarget effects of curcumin in breast cancer treatment. *Pharmaceutical Fronts*. 2025 (efirst);7(1):e41-52. <https://doi.org/10.1055/a-2522-0009>
17. Malla R, Viswanathan S, Makena S, Kapoor S, Verma D, Raju AA, Dunna M, Muniraj N. Revitalizing cancer treatment: Exploring the role of drug repurposing. *Cancers*. 2024 Apr 11;16(8):1463. <https://doi.org/10.3390/cancers16081463>
18. Deore S, Tajane P, Bhosale A, Thube U, Wagh V, Wakale V, Tare H. 2-(3, 4-dihydroxyphenyl)-5, 7-Dihydroxy-4H-Chromen-4-One flavones based virtual screening for potential JAK inhibitors in inflammatory disorders. *International Research Journal of Multidisciplinary Scope*. 2024;5(1):557-67. <https://doi.org/10.47857/irjms.2024.v05i01.0268>
19. Tajane P, Kayande N, Bhosale A, Deore S, Tare H. Design and discovery of silmitasertib-based drugs as a potential casein kinase II inhibitor for cholangiocarcinoma through hybrid in-silico ligand-based virtual screening with molecular docking method. *International Journal of Drug Delivery Technology*. 2023;13(4):1514-9. <https://doi.org/10.25258/ijddt.13.4.60>
20. Liu Y, Yang X, Gan J, Chen S, Xiao ZX, Cao Y. CB-Dock2: Improved protein–ligand blind docking by integrating cavity detection, docking and homologous template fitting. *Nucleic Acids Research*. 2022 Jul 5;50(W1):W159-64. <https://doi.org/10.1093/nar/gkac394>
21. Suvarchala Reddy NV, Ganga Raju M, Anusha V, Gaikwad A, Pulate C, Mahajan K, Tare H. Investigation of potential antiurolithiatic activity and in silico docking studies of Karpura shilajit. *International Journal of Health Sciences*. 2022;6(supplement 4):8900-16. <https://doi.org/10.53730/ijhs.v6nS4.11875>